Loss of brain norepinephrine elicits neuroinflammation-mediated oxidative injury and selective caudo-rostral neurodegeneration

Running title: Loss of norepinephrine and ascending neurodegeneration

Sheng Song[1*], Lulu Jiang[1,2*], Esteban A. Oyarzabal[1,3*], Belinda Wilson[1], Zibo Li[3], Yen-Yu Ian Shih[3], Qingshan Wang[1,4] and Jau-Shyong Hong[1]

1 Neuropharmacology Section, Neurobiology Laboratory, National Institute of Environmental Health Sciences, National Institutes of Health, Research Triangle Park, North Carolina, USA.

2 Institute of Toxicology, School of Public Health, Shandong University, Jinan, Shandong, China.

3 Biomedical Research Imaging Center, University of North Caroline at Chapel Hill, Chapel Hill, NC, USA.

4 Department of Toxicology, School of Public Health, Dalian Medical University, Dalian, Liaoning, China.

*=Denotes equal contribution with shared first authorship of this manuscript.

Correspondence to:

Jau-Shyong Hong, Ph.D. E-mail: hong3@niehs.nih.gov

Qingshan Wang, MD E-mail: Qingshan Wang (wangq4@126.com)

P.O. Box 12233

Mail Drop F1-01

Research Triangle Park, North Carolina 27709

U.S.A.

Supplementary Methods

Assessing neurodegeneration using traditional immunohistology. Free-floating sections either immunoblocked in 10% normal goat serum and incubated with polyclonal rabbit anti-TH antibody (CHEMICON, AB152, 1:4000) for 48 hours at 4°C or with 4% normal goat and horse serums and incubated with monoclonal mouse anti-NeuN antibody (CHEMICON, MAB377, 1:4000) overnight at 4°C. Sections were incubated with the biotinylated secondary antibodies for 1-2 hours. Antibody binding was visualized using a VECTASTAIN Elite ABC-HRP Kit (Vector Laboratories, PK-6100) and diaminobenzidine substrate.

Assessing neurodegeneration using double immunofluorescent histology. Free-floating sections were immunoblocked with 4% goat serum in 0.25% Triton-X/PBS for 2 hours and incubated with monoclonal mouse anti-NeuN antibody (1:2000) overnight at 4°C. Sections were washed twice for 20 minutes in 1% BSA in 0.25% Triton-X/PBS before incubating with polyclonal rabbit anti-TH antibody (1:2000) overnight at 4°C. Double-label immunofluorescence imaging was acquired using confocal microscopy of Alexa-488 conjugated anti-rabbit (Invitrogen, A-11034) and Alexa-594 conjugated anti-mouse (Invitrogen, A-11032) secondary antibodies (1:1000) to visualize the $NeuN^+$ and TH^+ neurons, respectively.

Assessing neurodegeneration using stereological counting methods. The number of TH^+ neurons in the SN*pc* was estimated using an optical fractionator method that systematically randomizes unbiased counting frames (100 µm × 100 µm) within defined boundaries of the SN*pc* (MBF Science, Stereo Investigator V11) [1]. Section thickness was determined in a pilot study that showed initial cut thickness at 35µm shrunk to about 20 µm after the staining process. A 11 µm dissector height was used and guard zone was set at 2 µm. Counts were done with an Olympus BX50 microscope using a 60 × 1.4NA oil immersion objective and the coefficient of error values was less than 0.1.

Assessing neurodegeneration using automated counting methods. $NeuN^+$ neurons in the DG, MCtx, and CPu were enumerated by automated counting in ImageJ using mono-colored immunographs [2]. Briefly, immunographs images were converted to gray scale and threshold adjusted to optimize to distinguish individual neurons. The binary watershed filter was used to separate clustered groups of neurons (by adjusting target particles size in attempts to reduce false-positive "noise" particles) and the total cell numbers were analyzed. Threshold and size parameters were consistently maintained among the images of all subjects.

PET imaging of glucose metabolism to assess neurodegeneration. Regional differences in [^{18}F]-fludeoxyglucose (FDG) tracer accumulation was measured on a GE eXplore Vista PET/CT. *In vivo* changes in FDG serves as a surrogate for brain activation since it reflects neuronal activity [3,4], synaptic function and densities [5,6] and astrocyte glutamate transport activity [7,8]. Mice were intravenously injecting ~10 MBq of the radiotracer [^{18}F]-FDG 45 min prior to imaging since the pharmacokinetic peak of brain [^{18}F]-FDG uptake requires ~30 minutes—which is dependent on cerebral metabolic rates of glucose, clearance from the circulation and radioactive decay. Mice were then scanned under 2% isoflurane for a 20 min PET static emission acquisition correcting for decay, attenuation, scatter and random

coincidences and a 6 min CT acquisition was collected for accurate skull stripping. Brain FDG images were aligned to an established mouse FDG atlas [9] with masks drawn over several brain regions that allow for the calculation of region-specific standardized uptake values (MBq/cm^3) that can be compared among subjects and displayed as an averaged three-dimensional projection for each treatment group by transforming them into normally distributed Z-scores in Amira (v5.2, FEI).

Densitometry of reactive microgliosis. The quantification of Iba-1 or CD11b immunohistological staining in SN, Hip, and MCtx was performed using the western blots quantification methods in ImageJ [10]. Briefly, Immunographs were converted to grayscale picture, the background adjusted before the quantifying area was selected for the measurement of the total pixels. The relative density of the staining was compared based on the density of the total pixels of a certain brain region (total pixels/area). Threshold parameters were consistently maintained among the images of all subjects.

Autoradiography and PET assessment of neuroinflammation. Mice were intravenously injected with ~10 MBq of the radiotracer [^{18}F]-PBR-111 45 min prior to imaging. Mice were then scanned under 2% isoflurane for a 20 min PET static emission acquisition correcting for decay, attenuation, scatter and random coincidences and a 6 min CT acquisition was collected for accurate skull stripping. Brain TPSO images were aligned to custom templates and regional standardized uptake values (MBq/cm^3) were and transformed into normally distributed Z-scores in Amira. The sensitivity and selectivity of TSPO was assessed by post-mortem autoradiography, whereby mice were euthanized immediately after their PET scans and their brains and quadriceps femoris muscle were collected and snap-frozen in liquid nitrogen. Three 14μm thick coronal sections were cut and evaluated at +1.00, -1.80 and -3.00 mm from Bregma and three sections of equal thickness were also extracted from the muscle tissue. Muscle tissue was used to establish a background threshold for [^{18}F]-PBR-111 uptake and their collective average standardized uptake value for each subject was set as the lowest threshold for brain tissue.

Effects of DSP-4 on Primary Neuron-Glia Cultures. Primary neuron-glia cultures consisting of neurons, microglia and astrocytes were prepared as previously described [11]. Briefly, the midbrain was extracted from E18 mouse embryos and dissociated into a single cell suspension that was seeded at 5×10^5/well and 1×10^5/well on poly-D-lysine-coated 24- and 96-well plates, respectively. Cell cultures were maintained at 37°C in a humidified atmosphere of 5% CO_2 and 95% air in minimum essential medium (Invitrogen, Grand Island, NY, USA) containing 10% heat-inactivated fetal bovine serum, 10% heat-inactivated horse serum, 1 g/L glucose, 2 mM L-glutamine, 1 mM sodium pyruvate, 100 μM nonessential amino acids, 50 U/ml penicillin, and 50 μg/ml streptomycin that was refreshed every four days. Seven days later, cultures were exposed to either 10 or 50 μM of DSP-4 or 20 ng/ml of LPS to compare with a known inflammagen. Supernatant was collected from 96-well plate cultures three hours following exposures to assess whether DSP-4 could directly activate microglia by detecting whether they released TNFα by ELISA using the manufacturer's instructions (R&D systems, MTA00B). Cultures in 24-well plates were fixed at 24 hours immunostained against Iba-1 to assess whether DSP-4-induced ramified morphological changes indicating their activation.

Rotarod test. The rotarod behavior test was measured using a Rotamex device (Columbus Instruments) [1]. The parameters of the rotarod system include start speed, acceleration, and highest speed (1 rpm, accelerate 12 rpm/2 s, 50 rpm). The mice underwent three consecutive trials. The rest period between each trial was 30 min. The mean latency time to fall off the rotating rod for the last two trails was used for the analysis.

Wire hang test. Mice were placed on top of a wire cage lid that was shaken gently 3 times, causing them to grip the wire. The wire cage lid was then inverted and suspended above the home cage. The latency to when the mice fall is recorded. The mice underwent two consecutive trials with 30 minutes' interval. The mean latency time to fall was used for the analysis.

Supplementary Figures and legends

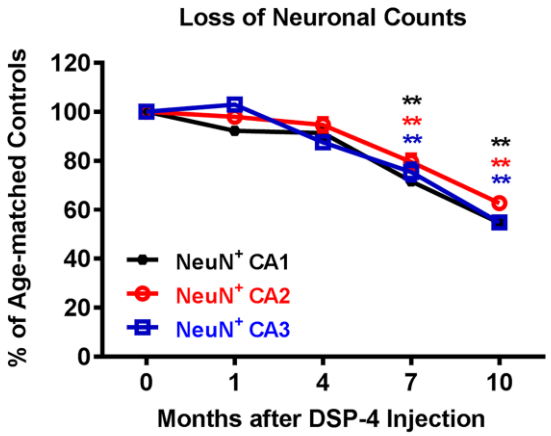

Supplementary Fig. 1 A single systemic injection of DSP-4 (50 mg/kg, i.p.) induced progressive degeneration of pyramidal layer neurons in the hippocampus. $NeuN^+$ neurons in the CA1, CA2 and CA3 pyramidal layers of the hippocampus were counted at 1, 4, 7 and 10 months following DSP-4 exposures and results were expressed as percentage neuronal loss compared to age-matched vehicle controls (n=4-6/group). Data are expressed as mean ± SEM. ** denotes $p< 0.01$.

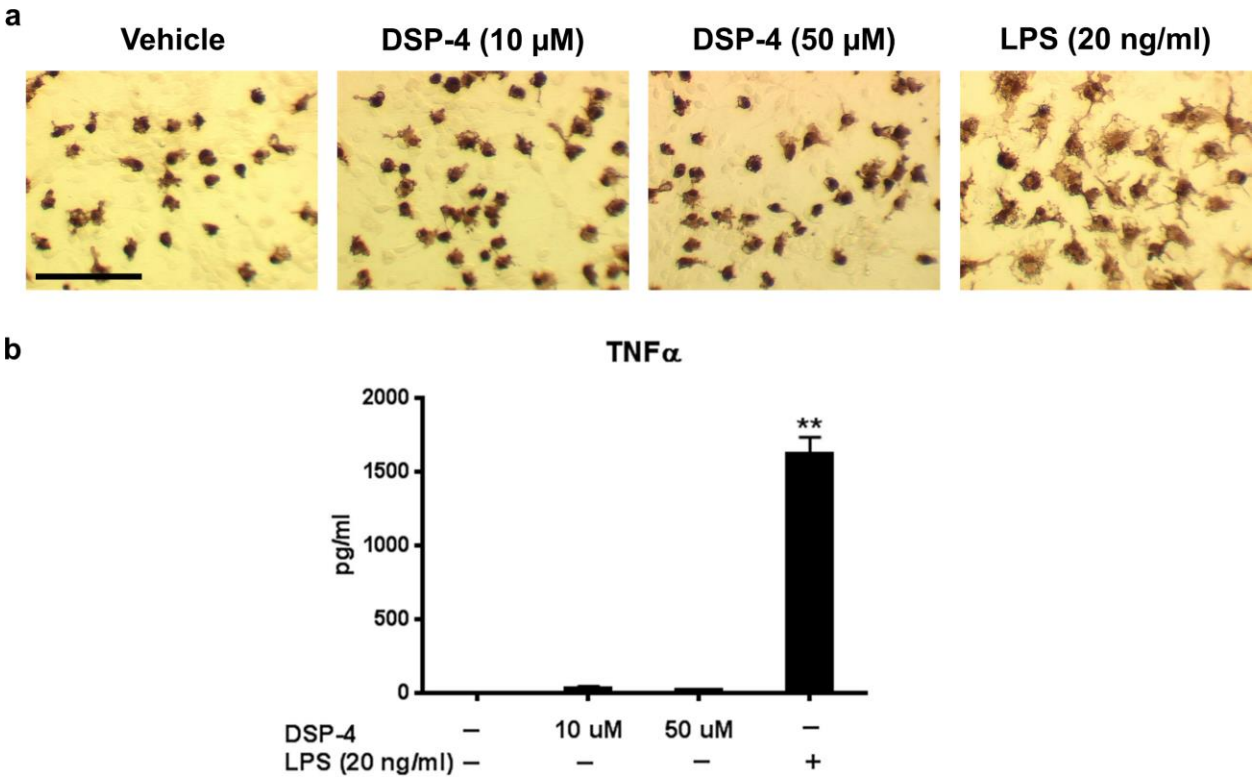

Supplementary Fig. 2 Treatment of primary midbrain neuron-glia cultures with DSP-4 for 24 hours fails to induce activation of microglia. (**a**) Immunocytochemical staining of Iba1^{+} microglia showed no change in microglial morphology following DSP-4 treatment, whereas LPS potently activated microglia (positive control). (**b**) Levels of TNFα in culture supernatants were not detectable at 3 hour following DSP-4 treatment, but showed significant elevation when exposed to LPS (positive control). Results are expressed as mean ± SEM from three experiments performed in duplicate. **denotes $p< 0.01$. Scale bar= 50 µm.

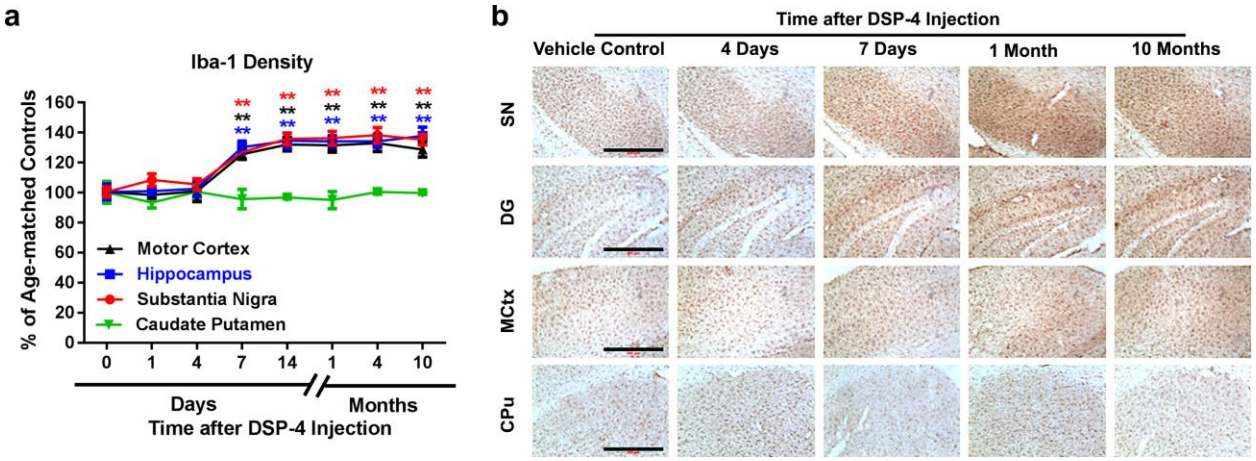

Supplementary Fig. 3 DSP-4 enhanced Iba-1 immunoreactivities (a marker for microglia) in brain regions innervated by noradrenergic locus coeruleus (NE-LC) neurons. (**a**) Changes in microglial morphology were assessed in the substantia nigra (SN), hippocampus (Hip), motor cortex (MCtx) and caudate/putamen (CPu) at 1, 4, 7 and 14 days and at 1, 4, and 10 months following an injection to age-matched vehicle control and DSP-4 (n=3-5/group) using an Iba1 antibody. Reactive microgliosis was assessed using Iba1 densitometry. Data are expressed as mean ± SEM. ** denoted $p<0.01$. (**b**) Representative immunostaining images of $Iba1^{+}$ microglia show significant morphological enhancement associated with reactive microgliosis in the SN, Hip, and MCtx, but not the Cpu, beginning at 7 days following DSP-4 injection. Scale bar= 300 µm.

References

1. Wang Q, Chu CH, Qian L, Chen SH, Wilson B, Oyarzabal E, Jiang L, Ali S, Robinson B, Kim HC, Hong JS (2014) Substance P exacerbates dopaminergic neurodegeneration through neurokinin-1 receptor-independent activation of microglial NADPH oxidase. The Journal of neuroscience : the official journal of the Society for Neuroscience 34 (37):12490-12503. doi:10.1523/JNEUROSCI.2238-14.2014

2. Cai Z, Chattopadhyay N, Liu WJ, Chan C, Pignol JP, Reilly RM (2011) Optimized digital counting colonies of clonogenic assays using ImageJ software and customized macros: comparison with manual counting. Int J Radiat Biol 87 (11):1135-1146. doi:10.3109/09553002.2011.622033

3. Attwell D, Iadecola C (2002) The neural basis of functional brain imaging signals. Trends Neurosci 25 (12):621-625

4. Sokoloff L (1977) Relation between physiological function and energy metabolism in the central nervous system. J Neurochem 29 (1):13-26

5. Rocher AB, Chapon F, Blaizot X, Baron JC, Chavoix C (2003) Resting-state brain glucose utilization as measured by PET is directly related to regional synaptophysin levels: a study in baboons. Neuroimage 20 (3):1894-1898

6. Sokoloff L, Reivich M, Kennedy C, Des Rosiers MH, Patlak CS, Pettigrew KD, Sakurada O, Shinohara M (1977) The [14C]deoxyglucose method for the measurement of local cerebral glucose utilization: theory, procedure, and normal values in the conscious and anesthetized albino rat. J Neurochem 28 (5):897-916

7. Zimmer ER, Parent MJ, Souza DG, Leuzy A, Lecrux C, Kim HI, Gauthier S, Pellerin L, Hamel E, Rosa-Neto P (2017) [18F]FDG PET signal is driven by astroglial glutamate transport. Nat Neurosci 20 (3):393-395. doi:10.1038/nn.4492

8. Stoessl AJ (2017) Glucose utilization: still in the synapse. Nat Neurosci 20 (3):382-384. doi:10.1038/nn.4513

9. Mirrione MM, Schiffer WK, Fowler JS, Alexoff DL, Dewey SL, Tsirka SE (2007) A novel approach for imaging brain-behavior relationships in mice reveals unexpected metabolic patterns during seizures in the absence of tissue plasminogen activator. Neuroimage 38 (1):34-42. doi:10.1016/j.neuroimage.2007.06.032

10. Gassmann M, Grenacher B, Rohde B, Vogel J (2009) Quantifying Western blots: pitfalls of densitometry. Electrophoresis 30 (11):1845-1855. doi:10.1002/elps.200800720

11. Wang Q, Qian L, Chen SH, Chu CH, Wilson B, Oyarzabal E, Ali S, Robinson B, Rao D, Hong JS (2015) Post-treatment with an ultra-low dose of NADPH oxidase inhibitor diphenyleneiodonium attenuates disease progression in multiple Parkinson's disease models. Brain 138 (Pt 5):1247-1262. doi:10.1093/brain/awv034